

Large Area Covering LiDAR Height Models – Problems and Solution

Gürçan Büyüksalih*, Karsten Jacobsen**

*BIMTAS, Istanbul, Turkey; buyuksalih@

**Leibniz University Hannover, Institute of Photogrammetry and Geoinformation, Germany;
jacobsen@ipi.uni-hannover.de

Abstract. The company BIMTAS, belonging to the Greater Istanbul Municipality, generates a digital height model (DHM) for the area of the Greater Istanbul Municipality with a Riegl LSM-Q680i full waveform laser scanner with 400kHz and a used field of view of $\pm 30^\circ$.

A precise absolute orientation requires ground control points (GCP), presented by height values of gable roofs to allow also an improvement of horizontal shifts. Because of the very high number of flight lines it is not possible to have GCP for any flight line, so sub-blocks of approximately 10 flight lines have been combined by 3D-transformation based on height points on planes. These sub-blocks have been transformed to the GCP. The varying overlap of neighbored LiDAR-strips in the range of 40% allows a three-dimensional transformation of neighbored, but if 10 strips of a sub-block are transformed together this may lead to unfavorable error propagation. The sub-blocks are only shifted to control point groups with points on inclined roofs and on the ground. Nevertheless a check of the transformed LiDAR-strips by check points results in a vertical accuracy of better as 5cm. Another possibility of joining overlapping LiDAR-strips is a filtering of the point cloud, eliminating points on vegetation and at building limits. Such a transformation uses quite more corresponding points as the method based just on planes and is robust also in areas only with few and not well distributed buildings. The result of transformation is on a similar level.

In addition to the original digital surface models (DSM) also DHM with the points of the bare ground have been generated.

The major problem of the LiDAR-points is the data amount. With a density of 16 points/m² a single strips has approximately 500 million ground points, exceeding the capacity of several programs.

Keywords. LiDAR, DEM generation, accuracy, filtering, handling, ortho image

1. Introduction

A digital surface model (DSM) with the height of the visible surface and a digital height model (DHM) with the height of the bare ground have been generated for the area of the Greater Municipality of Istanbul covering 5400km² by LiDAR based on a Riegl laser scanner Q680i with 400 kHz from 600m height as base for the generation of a 3D-city model. With 80kn, corresponding to 41m/sec, of the used helicopter, approximately 16 points/m² has been generated. Only over the international airport a flying elevation of 1250m had to be used, reducing the point density with different flight arrangement to approximately 12 points/m². From 600m flying elevation the laser footprint has a diameter of 30cm. Together with the laser scanner a mid-format camera IGI DigiCam 60 with 50mm focal length has been used for the generation of orthoimages.

2. Geometric handling and conditions

LiDAR point clouds are depending upon the direct sensor orientation and the boresight misalignment. The used relative kinematic GNSS positioning was based usually on at least 8 satellites with PDOP below 2.5. The processing indicated a standard deviation of the height (SZ) between 4cm and 7cm. Of course in addition there is the influence of the boresight misalignment which is not negligible. Crossing flight lines may be used for a block handling of LiDAR strips supported by ground control points (GCP), but such crossing flight lines are not available in this project and for the high number of flight lines GCP for every line are not realistic, so sub-blocks of approximately 10 flight lines have been built. With TerraMatch, included in TerraSolid, the approximately 50% overlapping neighbored point clouds of the different flight lines have been three-dimensionally transformed together and to control areas based on extracted inclined planes with at least 10° inclination. Such inclined planes, usually building roofs, allow not only vertical, but also horizontal fitting. Inclined planes are not affected by the not clear point definition of first return in vegetation areas and varying definition at facades where points with same horizontal positions may be located on the ground, on façade or even on overhanging roof.

The merged LiDAR point clouds have been analyzed with independent check points on a tennis court. The expected accuracy depends upon the standard deviation of the laser range of nominal $\pm 2\text{cm}$, the accuracy of the scan angle of $\pm 0.003^\circ$, the IMU roll and pitch of $\pm 0.003^\circ$, the IMU heading of $\pm 0.01^\circ$ and the relative kinematic positioning of $\pm 5\text{cm}$.

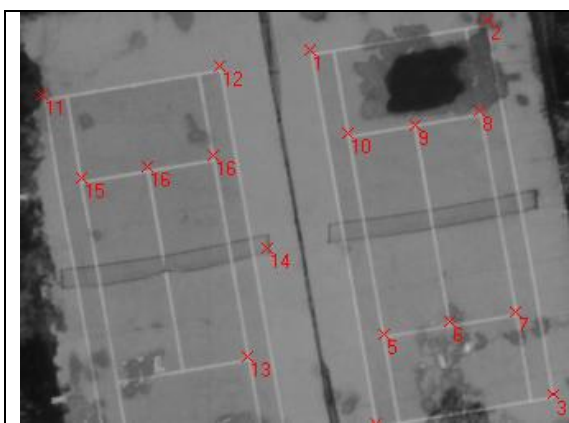


Figure 1: independent check points on a tennis court, shown in an ortho-image based on DigiCam

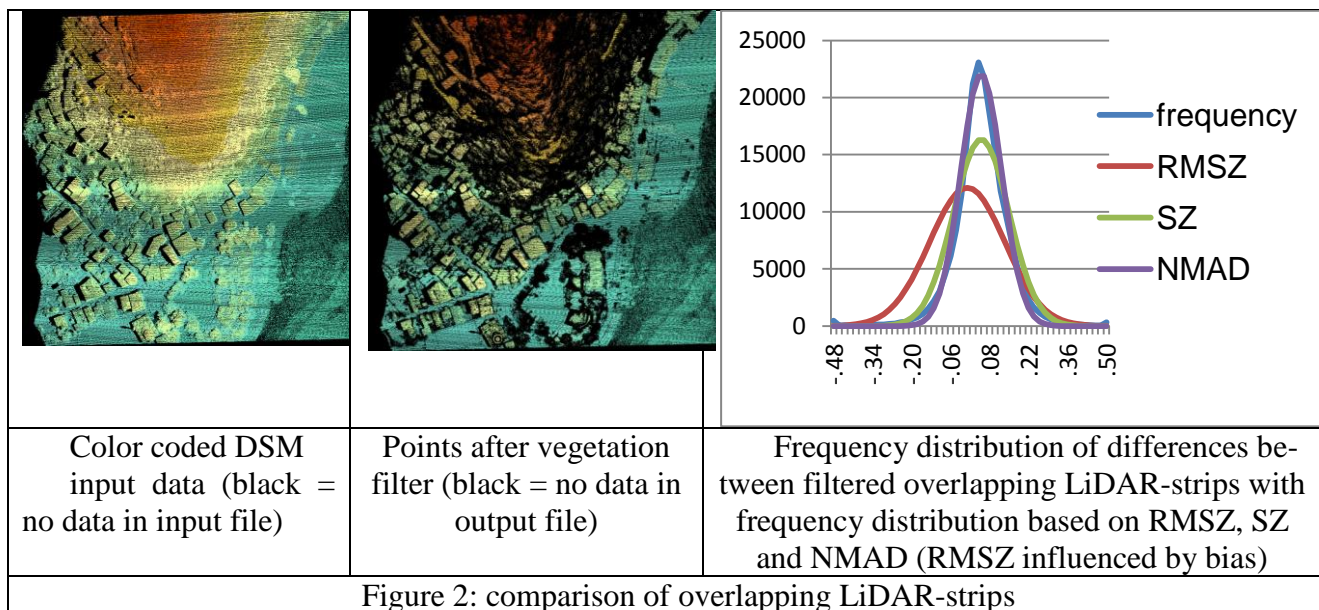
Lidar heights against check points: bias 0.003m, $SZ=0.033\text{ m}$

Height variation of the check points:
 $SZ_{\text{check}} = \pm 0.030\text{ m}$

Height variation of the Lidar points:
 $SZ_{\text{Lidar}} = \pm 0.014\text{ m}$

As shown beside figure 1 in this case there is nearly no bias of the LiDAR-points against the GPS reference measurement. Of course this only can be mentioned as a random result. On the other hand the root mean square differences of 3.3cm or even more the height variation of the LiDAR heights on the flat tennis court of just 1.4cm indicate at least high relative accuracy. The height variation of the GPS-heights of 3cm indicates a lower accuracy for the reference measurement as for the LiDAR-heights.

The direct comparison of overlapping LiDAR heights is dominated by the random influence of vegetation and at building outlines. By this reason the LiDAR point clouds have been filtered by a vegetation filter (Jacobsen 2013). Figure 2 shows a height model before and after vegetation filter. Based on the discrepancies standard deviations and normalized median absolute deviation (NMAD) have been computed. SZ and NMAD (Höhle and Höhle 2009) are identical if the discrepancies are normal distributed, but this is usually not the case (see also figure 2 right hand side including also the root mean square error (RMSZ)), more large discrepancies as corresponding to normal distribution exist, caused by remaining object roughness. NMAD describes in a better manner the frequency distribution of the observation, by this reason it should be preferred as accuracy figure against the standard deviation.



Strip combinations	SZ	NMAD	Influence of roll to Z from one side to other
1 - 2	0.06 m	0.05 m	0.025 m
2 - 3	0.10 m	0.09 m	0.028 m
3 - 4	0.11 m	0.10 m	0.040 m
4 - 5	0.05 m	0.04 m	0.000 m
5 - 6	0.05 m	0.04 m	0.029 m
8 - 9	0.12 m	0.10 m	0.210 m
9 - 10	0.08 m	0.06 m	0.050 m
8 - 9 after rotation correction	0.08 m	0.07 m	0.015 m

Table 2: discrepancies of overlapping Lidar DSM after vegetation filter

The comparison of strip 8 against 9 (table 2) indicates a clear rotation of the strips against each other. After correction of this rotation SZ and NMAD are more in the usual range of 6.3cm for NMAD and 7.9cm for SZ. These values are clearly larger as for the tennis court used as control area (figure 1), that means the dominating influence is caused by the object roughness – this is not a problem for strip transformation because the influence of the roughness dominantly is random and between 200 000 and 600 000 corresponding points have been used for analysis.

Another test of the LiDAR geometry is possible at the two airports in the project area. The concrete on the run- and taxi-way is flat and has only limited inclination, so directly neighbored points should have similar height values. In the area of the Atatürk airport the flying elevation was raised to approximately 4000 ft above mean sea level, corresponding to approximately 1200m above ground, while the Hezarfen airport was flown with the standard height of approximately 2000ft above mean sea level, corresponding to approximately 590m above ground. From the higher flying elevation lower height accuracy is expected. The comparison of neighbored points allows an analysis of the height measurement itself plus the influence of scene orientation after fitting neighbored strips together because directly neighbored points cannot be from the same LiDAR strip, they are belonging to different LiDAR-strips. The higher flying elevation is causing a reduced point density requiring a larger tolerance in horizontal location between corresponding points.

Test area	Points/m ²	Average point distance in DSM	Relative standard deviation for points with horizontal distance <0.10m	Relative standard deviation for points with distance <5m
1	8.3	35cm	8.6cm	12.7cm
2	7.2	37cm	7.6cm	9.1cm
3	7.9	36cm	10.7cm	9.6cm
4	9.5	32cm	6.1cm	5.6cm
5	11.6	29cm	5.2cm	4.7cm
<i>average</i>	<i>8.9</i>	<i>34cm</i>	<i>7.6cm</i>	<i>8.3cm</i>

Table 3: analysis of original height model Atatürk airport by relative standard deviation of ground points not exceeding listed distances

Test area	Points/m ²	Average point distance in DSM	Relative standard deviation for points with horizontal distance <0.02m	Relative standard deviation for points with distance <5m
1	27.2	19cm	1.3cm	5.6cm
2	16.5	24cm	1.5cm	6.1cm
3	26.1	25cm	3.2cm	6.9cm
4	15.8	25cm	0.8cm	5.0cm
<i>average</i>	<i>21.4</i>	<i>22cm</i>	<i>1.7cm</i>	<i>5.9cm</i>

Table 4: analysis of original height model Hezarfen airport by relative standard deviation of ground points not exceeding listed distances

Tables 3 and 4 present the results of the analysis at the run- and taxi-ways of Atatürk and Hezarfen airport. Of course from the higher flying elevation in the area of the Atatürk airport only 8.9 points/m² opposite to the Hezarfen airport with 21.4 points/m² have been achieved, but the tables mainly show the local height variation depending upon the coverage by more as one LiDAR strip.

The relative standard deviation of directly neighbored points (up to 10cm horizontal distance at Atatürk airport and up to 2cm at Hezarfen airport) show the accuracy of the distance measurement from the used helicopter and the remaining influence of strip orientation, while the relative standard deviation up to a distance of the points below 5m are combining also points from the same LiDAR strip. The analyses of points, with distances up to 5m, require flat and horizontal areas to reduce the influence of the terrain roughness.

For the lower point density of the Atatürk airport not a sufficient number of point combinations for distances below 2cm are available, requiring a limit of 10cm. The relative standard deviations in the area of the airport Atatürk is not as good as for the Hezarfen airport because of the higher flying elevation. With a point distance <2cm at the Hezarfen airport the same ground point has been determined, while with 10cm distance also slightly different points are used, having an overlap of the LiDAR footprints, but the first return may come from different objects located on the concrete plane.

The analysis of geometric height accuracy shows satisfying results. The relative height accuracy on flat terrain for the flying height up to 600m above ground is in the range of 1cm up to 2cm. Even the standard deviation of merging strips together for the height is not far away from this as shown by the relative standard deviation at Hezarfen airport. On not flat terrain the footprint of 30cm influences the results, enlarging the point definition accuracy to a standard deviation to 5cm up to 10cm.

3. Generation of DHM

Original LiDAR-height models are digital surface models (DSM) with height of the visible surface – on top of buildings and vegetation. For several cases digital height models (DHM) with height of the bare ground are required, so they have to be generated based on the DSM. The generation of DHM started with a classification of the area. With some macros from Terrasolid, allowing the classification for area types based on the LiDAR point clouds by some parameters, the area is classified into 5 classes – ground, buildings, low vegetation, high vegetation and noise. These classes have to be improved by manual editing. The height values of the classes low vegetation, high vegetation and buildings are erased from the DSM and the corresponding gaps are filled by interpolation from the neighborhood.

Figure 4 shows the situation of a DSM in relation to the DHM at a typical example. The DHM has been generated perfectly. Of course as in figure 4 the shape of the buildings partly can be seen in the DSM, but this is correct, because directly beside buildings the ground level is often elevated. In addition the ground height below buildings is a theoretical abstraction which has nothing to do with the reality because it is not showing the real height of the surface at the level of the basement, it just interpolates the neighborhood and this not in any case is unambiguous.

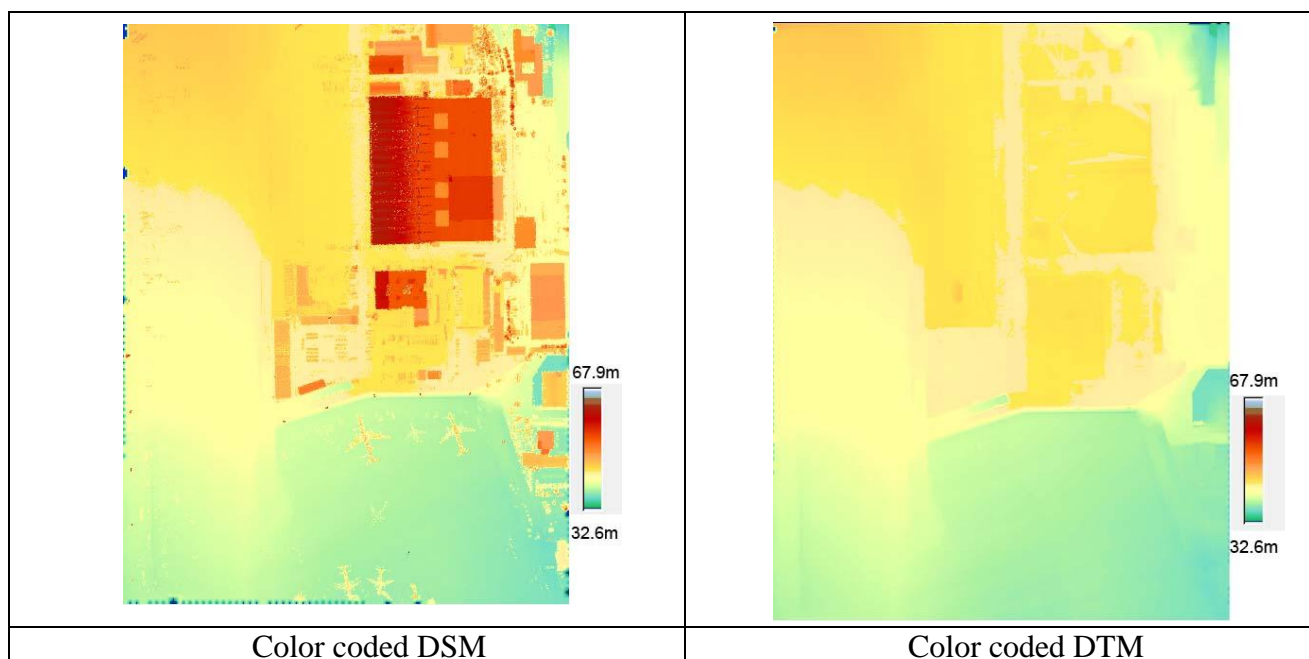


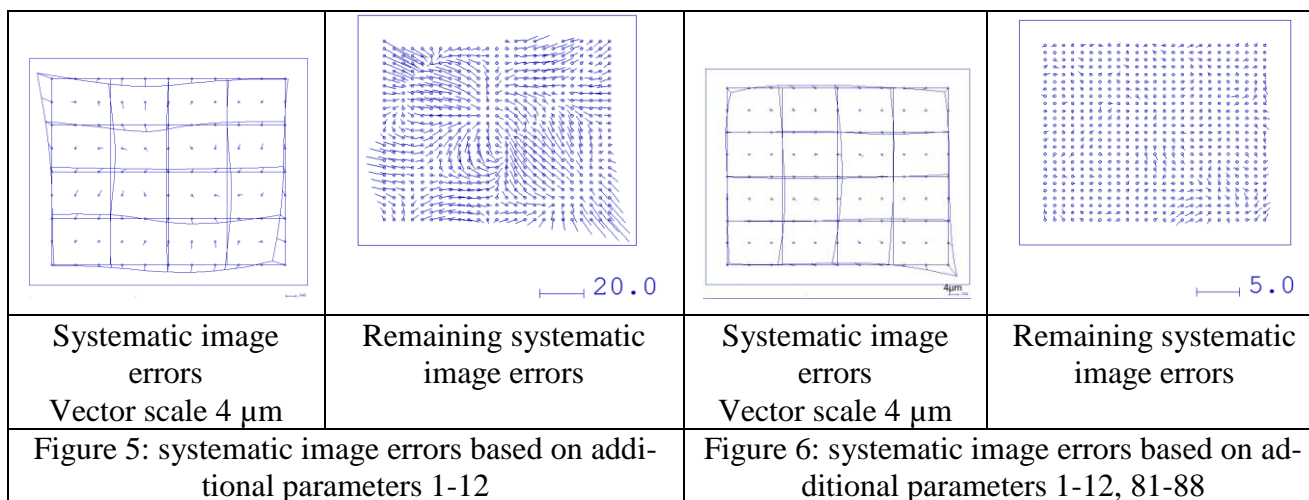
Figure 4: comparison of LiDAR DSM with DTM, Atatürk airport

Of course there are some objects where the DTM is not specified unambiguous – in the case of bridges with heights on top of bridges walls are caused for the lower level or gaps for the higher level if the height is defined for the lower level. Such a problem cannot be solved with the usual 2.5-D height models where only one height is specified corresponding to the X- and Y-location.

4. Orthoimages

Together with the laser scanner a mid-format camera IGI DigiCam 60 with 50mm focal length was used for the generation of orthoimages. The geometry of the camera has been investigated with a block of images based on automatic aerial triangulation by TerraPhoto supported by direct sensor

orientation. Not all images could be used in the block adjustment because in forest areas the tie point generation failed. Such areas have been bridged by means of the direct sensor orientation.



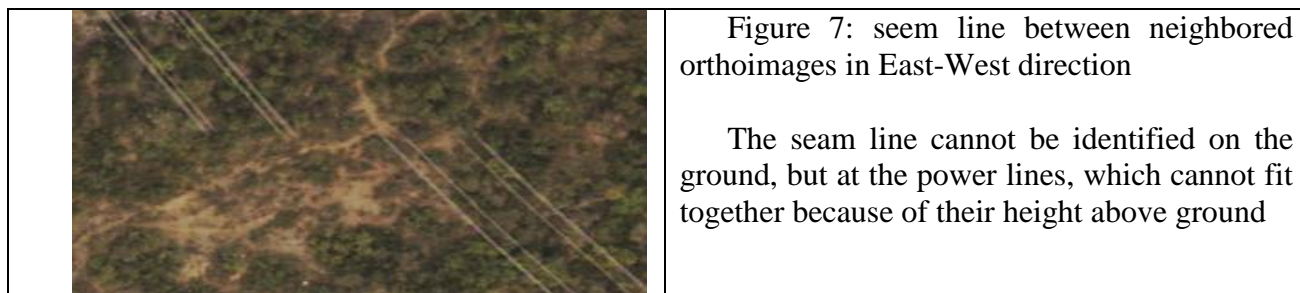
With the standard set of additional parameters 1 – 12 in Hannover Program BLUH the σ_0 is reduced to 10.97 μm . The large values of the remaining systematic image errors (figure 5, right) indicates clear problems at the image corners, requiring the special additional parameters for image corners 81 – 88. If the special additional parameters for the image corners are added, σ_0 drops to 7.85 μm , but the handling of the block adjustment with the GPS-projection centers requires also the use of the additional parameters 13-15 for the inner orientation (13 = correction of focal length, 14 and 15 = corrections for the principal point in x and y-direction). With the set of additional parameters 1-15 and 81-88 σ_0 drops down to 4.88 μm . Under the condition of the automatic aerial triangulation just for image tie to fit orthoimages together, this is an acceptable result.

The additional parameters 81 – 88 are respecting the remaining systematic image errors (figure 5, right) by changing the systematic image errors especially in the upper left and lower right corner. With the exception of these corners the systematic image errors have a limited size in the root mean square of just 0.9 μm for x and 0.7 μm in y with the maximal component of 4.8 μm . The remaining systematic image errors are limited within the root mean square average of +/-0.6 μm for x and y, with maximal 2.8 μm . Such differences are small for mid-format cameras. The systematic image errors of up to 4.8 μm (0.8 pixels) in the extreme corners are not a problem because images are overlapping and usually they are used only approximately up to the centre of overlapping area so that the distortion in the extreme edges are not disturbing.

Against independent check points root mean square X- and Y-values of 11.3cm and in the height 20.5cm have been reached. This is totally satisfying for orthoimages with 10cm GSD based on images with in maximum +/-28° field of view.

The ortho images have been generated with TerraPhoto belonging to Terrasolid. TerraPhoto can determine seam lines operator supported automatically. By color balancing brightness, contrast and color differences between neighboring images are eliminated to avoid disturbing radiometric changes from one image to the next.

The seam lines between neighbored images are somewhere in the individual ortho images which are cut by coordinate lines. The ortho images are based on the DHM, so the geometry can be correct only at the height level of the DHM – that means the bare ground.



The misfit of the power lines in figure 7 cannot be avoided because they are not located on the height level of the DHM and removing by selected seam lines is not possible because power lines do not have a limited size as for example buildings. By means of the power lines the seam line location could be identified – this was not possible without such a support because the radiometric property of neighbored ortho images was well fitted and no misfit in the ground level can be seen. Similar it was for all seam lines, they cannot be identified without additional information that means a very good radiometric and geometric fit was made.

5. Conclusions

The used strategy for generating homogenous high quality DSM and DHM by LiDAR from a helicopter was successful. The transformation of sub-blocks of LiDAR-strips together, without crossing flight lines, was without problems. The different tests confirmed the high accuracy level, which is mainly limited by the object itself – a rough terrain cannot be specified with an accuracy of 1cm up to 2cm, here the accuracy is limited to 5cm up to 10cm.

The orthoimages based on the mid-format camera and the DHM are optimal, the very small systematic image errors of the IGI DigiCam 60 with 50mm focal length did not cause problems. The seam lines between neighbored orthoimages are optimal. Together with the automatic radiometric fit the seam lines could not be identified without additional information as it is available in case of power lines, not located in the height level of the DHM.

References

- [1] Höhle, J., Höhle, M., 2009: *Accuracy assessment of digital elevation models by means of robust statistical methods*, ISPRS Journal of Photogrammetry and Remote Sensing, 64, pp. 398-406
- [2] Jacobsen, K., 2013: *Characteristics of Airborne and Spaceborne Height Models*, EARSeL Symposium Matera, 2013, <http://www.earsel.org/symposia/2013-symposium-Matera/proceedings.php>